

Effects of control structure on performance for an automotive powertrain with a continuously variable transmission

Sharon Liu, Anna G. Stefanopoulou

Abstract—The wheel speed control problem of an automotive powertrain equipped with a conventional spark-ignition engine directly connected to a continuously variable transmission (CVT) and an electronic throttle is considered. We revisit the seminal work by Guzzella & Schmid, 1995 and show that the control structure that dedicates the throttle actuator to maintaining engine operation at the maximum fuel efficient operating points results in a single-input, two-output (SITO) system that presents a fundamental limitation in the achievable wheel speed response. The limitation arises from the nonminimum phase (NMP) zero in the transfer function from the CVT ratio rate to the vehicle wheel speed. We relax the requirements on the fuel efficient operation and employ the electronic throttle as a second actuator for the wheel speed regulation problem. The resulting two-input, two-output (TITO) control structure is then analyzed to determine how to mitigate the limitations associated with the NMP zero. Simulations show that the multivariable strategy improves the system performance because it produces minimum phase behavior without large transient deviations from the optimal fuel economy operation.

Keywords— controller structure, continuously variable transmission powertrain, automotive control, performance limitations.

I. INTRODUCTION

MANY continuously variable transmission (CVT) designs are being realized in the automotive industry today: [1], [2] use variable stroke drives; [3] designs a nutating tractive drive; [4] develops a toroidal tractive drive directly connected to a spark ignited (SI) engine; [5] interfaces a variable speed pulley drive with an electromagnetic clutch; [6] connects their pulley drive directly to the SI engine; [6]-[8] have pulley drives designed with conventional hydraulic torque converters; [9] puts a pulley drive behind a diesel engine, and [10], [11] use a pulley drive in a hybrid electric vehicle. A historical perspective of CVT mechanical development is in [12].

While the mechanical development of CVT devices has matured, CVT powertrain control design is still actively being researched. Together with the use of electronic throttle actuators, the primary benefit of CVT devices, its continuously varying ratio, lets the engine operate independently of any load. In principle, this flexibility allows the fuel economy to be optimized without degrading the acceleration performance [13]. But optimizing every operating condition, from launch to engine braking, is not trivial [6],

[14], [15]. The experienced observations of [16] suggest potential for improvements in the CVT controls.

When electronic throttle actuators are used, a strategy is needed to convert the driver pedal position input into an operating command [6], [14], and [15]. The strategy can be a static feedforward map from pedal position to the desired vehicle performance. A fuel economy objective can then be used to determine the desired engine operation corresponding to the desired vehicle performance through an appropriate choice of the CVT ratio. The literature covers many different strategies [6], [7], [8], [9], [10], [14], [15], [17].

The desired CVT powertrain transient specifications are usually determined for different performance objectives, and always include either a warning to monitor ([4], [6], [14]) or limits on ([15], [7]) the CVT ratio rate. This is because the wheel speed equation of motion shows that the ratio rate input opposes the throttle input. This characteristic is equivalent to a nonminimum phase (NMP) zero in the transfer function from the ratio rate input to the wheel speed output when the system model is linearly approximated [10]. NMP behavior is undesirable because, first, the initial transient step response of a stable linear system with one real NMP zero starts in the wrong direction, has initial undershoot. Second, feedback cannot remove NMP zeros. And third, open-loop systems with NMP zeros have closed-loop performance limitations that are well documented, i.e. [18], [19], and their references. Hence, to achieve all desired control objectives, the engine and CVT subsystems must be dynamically coordinated [8].

Some commercial applications avert any NMP behavior by employing additional power sources to compensate the initial inverse response. For example, [26] and [27] use energy stored in a flywheel to passively compensate for the initial inverse wheel speed response. Using nonlinear inverse dynamics, [25] cancels the ratio change effect on the wheel speed with the electric motor in the ETH hybrid electric powertrain. In a different discussion about this Hybrid Electric Vehicle, fuel efficiency is maximized by dedicating the throttle actuator to controlling the engine on a fuel optimum speed-load trajectory. The ratio rate is then used solely to govern the vehicle acceleration. To avoid bandwidth limitations associated with the NMP response of the output feedback (SISO), [10] uses a nonlinear state feedback (SITO architecture).

The first result we present here clarifies that the initial inverse response cannot be eliminated by using additional

Sharon Liu is with Advanced Propulsion System Controls, General Motors Powertrain, Milford, MI, USA. E-mail: sharon.liu@gm.com .
Anna G. Stefanopoulou is with the Department of Mechanical Engineering, University of Michigan, Ann Arbor, MI, USA.

measurements and the undesirable behavior persists unless the ratio rate is detuned considerably. It is thus shown that the controller architecture that dedicates the throttle actuator to ensure the fuel economy objectives and the CVT to meet the driveability objectives presents a stringent trade-off between the fast wheel speed response and initial monotonic wheel speed response. To mitigate this tradeoff we relax the transient fuel economy requirements and investigate if a TITO controller that coordinates both throttle and ratio rate commands can achieve better driveability performance. Since it is well known that the multivariable (MIMO) controller structure plays an important role in achieving a better trade-off between various performance objectives when fundamental limitations are present [20], [23], we investigate a decentralized and a fully centralized (multivariable) controller structure.

Our second result is that a low order decentralized TITO controller *cannot* alleviate the above tradeoff between fast and monotonic wheel speed response associated with the NMP zero, unless the throttle can affect engine torque instantaneously. This is unrealistic with conventionally throttled gasoline engines, hence, we postulate that a fully multivariable (centralized) TITO structure is a better solution.

Our final result shows that, indeed, the multivariable controller structure provides the degrees of freedom to achieve fast and monotonic wheel speed response. In addition, we identify the exact mechanism with which a cross coupling term of the multivariable controller achieves the performance objectives.

Our results are independent of control design methodology and specific plant (engine/CVT) parameters. Thus, they can be used early in the system design process. The design implications of our controller structure analysis can be summarized as follows. One should not relax the transient fuel economy requirements if a coordinated (multivariable) TITO controller structure cannot be used in the final vehicle implementation. It is also evident that one should explore the inexpensive software solution of the multivariable controller structure before increasing the mechanical system complexity by employing a supplemental torque source configuration (electric motor, flywheel, etc) in order to alleviate the initial inverse wheel speed response.

This paper is organized as follows: The assumptions used to model the system of interest, the control objectives, and the derivation of the system open-loop state space are presented in Section III. Since the electronic throttle actuator is coordinated with ratio rate as an input, the engine breathing dynamics is also modeled. The relationship between the desired optimum fuel consumption trajectory, the driver input interpretation, and the state tracking reference is explained in Section IV. The linearization of the model about the reference steady states result in a two-input/two-output (TITO) realization described in Section V. Constraining the engine to operate on the optimum fuel consumption trajectory at all times reduces the TITO system to a single-input/two-output (SITO) problem. The resulting limitations for this approach are discussed in Sec-

tion VI. To overcome some of these limitations, the TITO system is constrained to operate on the optimum fuel consumption trajectory only at steady state. Low order decentralized and multi-variable controllers are applied to the TITO system, in Section VII, and their ability to achieve the control objectives are compared. Examples of closed-loop responses to “kick-down” commands are included in this section. They illustrate the role of the closed-loop architecture in the inevitable trade-off between wheel acceleration performance and fuel economy. Conclusions and suggestions for future investigations are discussed in Section VIII

II. NOMENCLATURE

r	powertrain speed ratio
ω_e	engine speed
ω_w	wheel speed
T_{eb}	brake engine torque
T_w	wheel torque
T_{ind}	indicated torque
c_{ef}	co-efficient of engine friction
I_e	engine inertia
I_w	effective car inertia at the wheels
$c_{1,2,3,4}$	constant polynomial coefficients
m_a	cylinder air charge mass
τ_{bd}	engine breathing dynamics time constant
ϑ	throttle command
β	driving surface incline
C_F	tire friction coefficient
C_D	air drag coefficient
T_l	effective vehicle torque load
W_c	vehicle weight
OOL	optimum operating line
$\Gamma(\omega_e(t))$	specific OOL
x^o	desired steady state value
α_p	driver pedal position
$\tilde{\alpha}_p$	scaled driver pedal position
\mathbf{S}_I	sensitivity transfer function
\mathbf{T}	complementary sensitivity transfer function
rd	relative degree

III. MODEL

Standing assumptions for the system are:

- a spark-ignition internal combustion engine generates power
- a CVT directly connects the engine to the wheels
- the CVT device is modeled as an integrator based on the assumption that an internal controller generates its response
- there is no slip across the powertrain

The first three assumptions coincide with the conditions imposed in [10]. The last assumption ensures that Eq (1) holds. Let the powertrain speed ratio be defined as

$$r = \frac{\omega_e}{\omega_w} = \left(\frac{T_{eb}}{T_w}\right)^{-1} \quad (1)$$

where ω_e is the engine speed, ω_w is the vehicle wheel speed, T_{eb} is the brake engine torque, and T_w is the wheel torque. Notice that when the engine brake torque is zero, and the vehicle speed is zero, for example when the engine idles with zero vehicle speed, the speed ratio is infinite in Eq (1). Operations near this condition will not be addressed.

The powertrain model is based on the relationship described by Eq (1). The brake engine torque, T_{eb} , is the indicated engine torque, T_{ind} , minus frictional losses and the inertial torque. The indicated engine torque can be approximated as a function that is linear in the mass of air charge into the cylinders, m_a , and is quadratic in the engine speed, ω_e ,

$$\begin{aligned} T_{eb} &= T_{ind} - c_{ef} \omega_e^2 - I_e \dot{\omega}_e \\ T_{ind} &= c_1 + c_2 m_a + c_3 \omega_e + c_4 \omega_e^2 \end{aligned} \quad (2)$$

For the analysis, the manifold filling dynamics, throttle actuator dynamics, and induction to power delay are lumped into a single linear first order lag, with time constant $\tau_{bd} = 0.07$ s, from the throttle command, ϑ , to the cylinder air charge, m_a ,

$$\dot{m}_a = \frac{1}{\tau_{bd}} (\vartheta - m_a). \quad (3)$$

Note that if we assume the worst case pure time delay for the slowest engine speed of interest to be 0.03 s then a lag of 0.027 s in series produces the same phase lag as the 0.07 s time lag we use in our analysis and simulations. Additionally, the rational Pade approximation of a time delay does not change the relative degree arguments that we employ in the following analysis in Sections VI-VII.

The tractive torque in Eq (1), T_w , drives the wheels, and includes the vehicle load. The vehicle load consists primarily of air drag, vehicle weight on the driving surface incline, β , and tire friction resistance [22]. The tire friction coefficient, C_F , air drag coefficient, C_D , and the vehicle weight, W_c , have known nominal values. Only the forward driving operations are considered,

$$\begin{aligned} T_w &= I_w \dot{\omega}_w + T_l \\ T_l &= C_F W_c \cos \beta + W_c \sin \beta + C_D \omega_w^2. \end{aligned} \quad (4)$$

Using the time derivative of Eq (1), $\dot{\omega}_e = r \omega_w + r \dot{\omega}_w$, then substituting expressions from Eq (2), (3), and (4) into Eq (1), the wheel acceleration can be solved in terms of wheel speed (see Appendix). The system state space is described in Eq (5) when the ratio, the wheel speed, and the cylinder air charge are chosen as states, $x = [r \ \omega_w \ m_a]^T$, and the ratio rate and the command throttle are chosen as inputs,

$$u = [\dot{r} \ \vartheta]^T.$$

$$\dot{x} = \begin{bmatrix} f_1 \\ f_2 \\ f_3 \end{bmatrix} + \begin{bmatrix} 1 & 0 \\ g_1 & 0 \\ 0 & \frac{1}{\tau_{bd}} \end{bmatrix} u, \quad y = \begin{bmatrix} r \\ \omega_w \end{bmatrix}$$

$$\begin{aligned} f_1 &= 0 \\ f_2 &= \frac{[(c_4 - c_{ef}) x_1^3 - C_D] x_2^2 + c_3 x_1^2 x_2 + [(c_1 + c_2 x_3) x_1 - \bar{\beta}]}{I_w + I_e x_1^2} \\ f_3 &= -\frac{1}{\tau_{bd}} x_3 \end{aligned} \quad (5)$$

$$g_1 = -\frac{I_e x_1 x_2}{I_w + I_e x_1^2}, \quad \bar{\beta} = C_F W_c \cos \beta + W_c \sin \beta$$

The state equation for wheel acceleration, \dot{x}_2 , shows that the ratio rate input, u_1 opposes the throttle input or mass air charge response, $x_3 = m_a$, because $(c_1 + c_2 x_3) x_1$ is positive for all x_1 and x_3 , and g_1 is negative for all $I_e x_1 x_2$, in the forward driving range. The control problem is to track the desired wheel speed and ratio. The desired steady state conditions are discussed in the next section.

IV. OPTIMUM OPERATIONS

We consider a small “kick-down” maneuver as the evaluation criteria, similar to [10]. This maneuver is a driver imposed acceleration demand that requires both an engine torque increase and a transmission ratio change. The closed-loop control objective is to achieve stable, monotonic wheel speed response with zero steady state tracking error to a “kick-down” command.

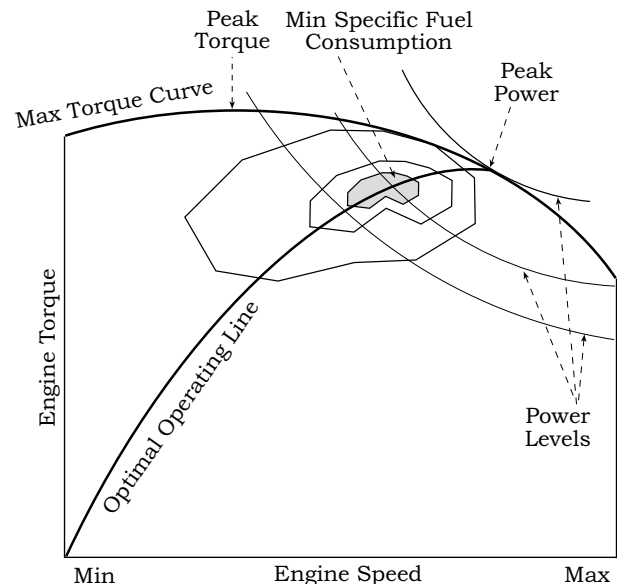


Fig. 1. The optimal operating line (OOL) on a generic engine characteristics map

Moreover, we consider a line that represents the minimum brake specific fuel consumption for every brake engine power level on the generic engine characteristics map shown in figure 1. This line is coined the optimum operating line (OOL) in [21] because, in general, it can be chosen to represent the ideal engine operations prescribed by

the powertrain designer. For convenience, the term OOL is adopted here. For consistency with [10], the OOL is defined as $\Gamma(\omega_e(t))$; to achieve maximum fuel efficient operations, the desired steady state engine operating points are along $\Gamma(\omega_e(t))$.

The OOL can be described by a one-to-one map of the desired steady state engine speed, ω_e^o , and the desired steady state engine torque, $T_e^o = \Gamma(\omega_e(t))$. This trajectory is always maintained by some control strategies, such as [10]. It is used only as the desired steady state reference trajectory in the current study. For example, if the driver pedal position input, α_p were interpreted as a desired power level, [6], then the desired steady state engine speed, ω_e^o , and the desired steady state mass air flow, m_a^o , can be found by using the definition of power, $\Gamma(\omega_e(t))$, Eq (2), and (3). With no slip across the powertrain, the desired engine power is equal to the desired output power at the wheels. Therefore, using the definition of power with Eq (1) and (4), the desired steady state wheel speed, ω_w^o , and the desired steady state ratio, r^o , are determined. In the following linearization and analysis, $C_o = [\alpha_r \ 1]^T$ is the smooth transformation which maps the scaled driver pedal position input or command, $\tilde{\alpha}_p$, to the reference state, $[r^o \ \omega_w^o \ m_a^o]^T = x^o$.

V. LINEARIZATION

The transfer function of Eq (5) linearized about the steady state x^o is

$$P(s) = \begin{bmatrix} \frac{1}{s} & 0 \\ \frac{(g_1(x^o)s + \frac{\partial f_2}{\partial x_1}|_{x^o})}{s(s - \frac{\partial f_2}{\partial x_2}|_{x^o})} & \frac{\frac{\partial f_2}{\partial x_3}|_{x^o} \frac{1}{\tau_{bd}}}{(s - \frac{\partial f_2}{\partial x_2}|_{x^o})(s + \frac{1}{\tau_{bd}})} \end{bmatrix}. \quad (6)$$

The controller inputs are the ratio rate and the throttle command. The measured outputs are the ratio and wheel speed. For all x^o , $g_1(x^o) < 0$; $\frac{\partial f_2}{\partial x_1}|_{x^o} > 0$; $\frac{\partial f_2}{\partial x_2}|_{x^o} < 0$; $\frac{\partial f_2}{\partial x_3}|_{x^o} > 0$; $\tau_{bd} > 0$.

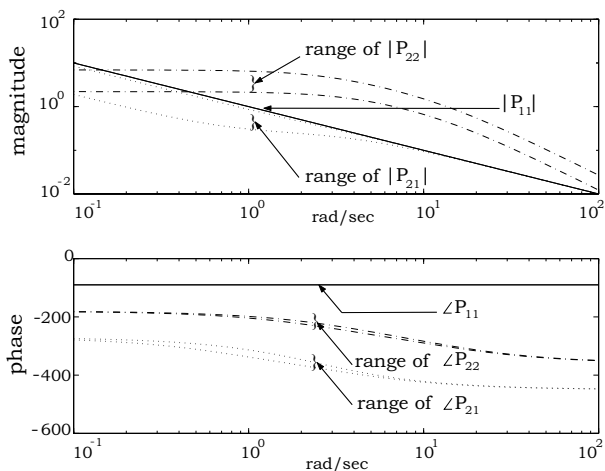


Fig. 2. Bode plots of the transfer function elements in Eq (6)

There is a NMP zero in P_{21} which maps $\dot{r} \rightarrow \omega_w$. This is apparent in the Bode plots of the individual transfer

functions from Eq (6) shown in figure 2 for $\alpha_p = 0.1$ and 0.99. The phase for $\angle P_{21}$ is not minimum, with an additional 90 degrees lag. However, the coprime factorization of Eq (6), contains no multivariable transmission zeros. The frequency gain plot in figure 2 shows that there is considerable interaction between the impulse response of each output to each input and that the bandwidth of P_{22} is important for rejecting the disturbances from the CVT dynamics. These open-loop characteristics for Eq (6) represent a two-input/two-output (TITO) structure, from the ratio rate and throttle inputs to the ratio and wheel speed outputs. In the next section we show how the authors in [10] formulate a SITO control problem by dedicating the throttle actuator to ensure engine operation at the OOL. We also analyze the pertinence of the SITO architecture limitations.

VI. SITO ARCHITECTURE

The optimum fuel objectives are achieved if the engine torque satisfies $T_e(t) = T_e^d = \Gamma(\omega_e(t))$. The electronic throttle, ϑ , can be controlled to ensure that the engine torque tracks this desired Γ curve for all engine speeds. Similar to figure 2 in [10], figure 3 illustrates the architecture for this approach. The authors there use an instantaneous mass of air charge response, m_a , to the command, ϑ that satisfies $T_e(t) = \Gamma(\omega_e(t))$ based on Eq (2) and (3). The throttle control, C_2 , reacts only to changes in the engine speed caused by the drivetrain, through CVT command or load disturbances. Due to the inertial rotational dynamics, these changes in engine speed are much slower than the engine breathing or combustion dynamics, $\vartheta \rightarrow T_e$. Hence, by the principle of frequency separation, a fast closed-loop system in m_a can easily track the slowly varying $\Gamma(\omega_e(t))$ trajectory and maintain engine operation on the OOL, i.e. maintain $T_e(t) = \Gamma(\omega_e(t))$. The control problem is then posed by a SISO wheel speed tracking problem controlled by the CVT ratio rate.

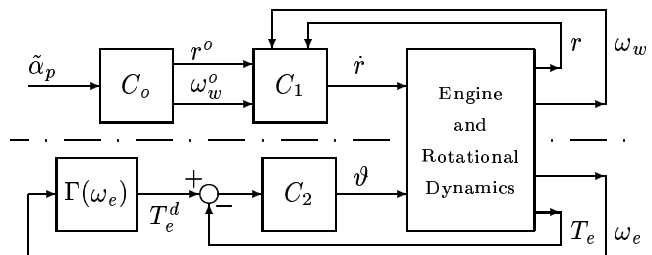


Fig. 3. The CVT powertrain control system block diagram

Guzzella & Schmid avoids the closed-loop bandwidth limitations associated with the NMP zero by utilizing an additional measurement, namely, the CVT ratio, to form the SITO system shown in figure 4. This SITO system does not have NMP MIMO transmission zeros, thus there is no bandwidth limitation associated with the SITO plant. However one can show that any stable closed-loop transfer function from $\tilde{\alpha}_p$ to ω_w that uses \dot{r} for the single actuator will still have the NMP zero. Thus the wheel speed will

exhibit the undesirable inverse response even when extra sensors are employed. Recall that internal stability of the feedback system prohibits cancellation of the NMP zero. The complementary sensitivity function of the system in figure 4 shows that the NMP zero must affect the wheel speed independently of the control algorithm for \dot{r} ,¹

$$\begin{aligned} \frac{\omega_w}{\tilde{\alpha}_p} &= P_{21}(1 + C_{12}P_{21} + C_{11}P_{11})^{-1}(\alpha_r C_{11} + C_{12}) \\ &= P_{21}\mathbf{S}_I(\alpha_r C_{11} + C_{12}) \\ &= \mathbf{T}. \end{aligned} \quad (7)$$

Where $z > 0$ is the real NMP zero, $\mathbf{T}(z) = 0$ and $\mathbf{S}_I(z) = 1 - \mathbf{T}(z) = 1$. Due to the interpolation constraints, the wheel speed step response will satisfy the following relationship,

$$\int_0^\infty e^{-zt} \omega_w(t) dt = 0. \quad (8)$$

Since $e^{-zt} > 0$, it follows that $\omega_w(t) < 0$ for some time interval so that the wheel speed will exhibit undershoot. The above holds for all control signals that are bounded integrable functions. Per [24] the undershoot is unavoidable even if the controller is nonlinear or time varying.

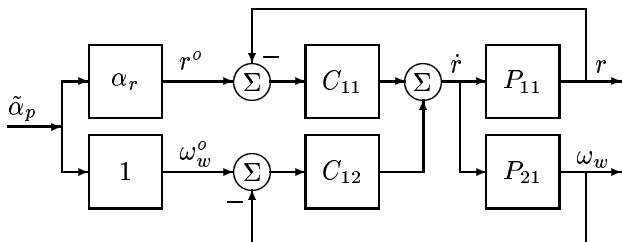


Fig. 4. The SITO form of figure 3

Moreover, the Poisson integral constraints hold and impose sensitivity peaking to counterbalance the aggressive sensitivity decrease at some frequencies. This sensitivity peaking needs to be carefully assessed both in terms of stability and transient performance.

While adding measurements for the inner loops may not remove the NMP behavior, changing the powertrain control strategy does. By relaxing the requirement of engine operation at the OOL curve ($T_{eb} = \Gamma(\omega_e)$), the throttle, ϑ , can be used as an additional actuator for tracking the desired wheel speed. Fuel efficiency is thus traded for drivability. The throttle now must be coordinated with the CVT ratio rate and the breathing dynamics becomes important because the engine torque is used to compensate fast transient wheel acceleration.

The 3rd order TITO system of interest is given by Eq (5). The effects of the choice of the multivariable controller architecture on the TITO system performance are investigated in the next section.

¹Dependence on the complex variable s has been omitted for legibility.

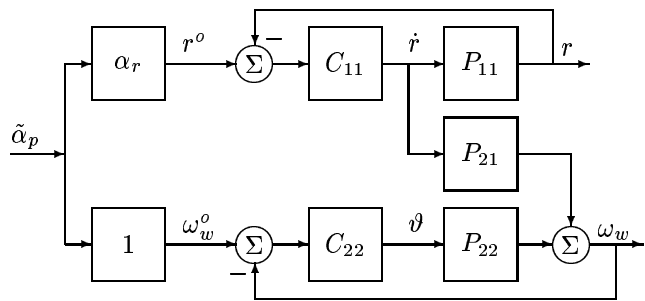


Fig. 5. The decentralized controller with the TITO system

VII. EFFECTS OF TITO CONTROLLER STRUCTURE

In the previous section we show that the coordination of throttle and ratio rate might be critical in alleviating the inverse response of the wheel speed. Significant coupling of the resulting system at the frequencies of interest is shown by the Bode plots in figure 2. This suggests that a fully centralized multivariable controller has the capability to coordinate both throttle and ratio rate.

To verify this hypothesis, we specifically investigate a multivariable controller based on the wheel speed and ratio error in a unity feedback configuration. This configuration is practically the automotive industry standard. Another automotive industry standard is the use of decentralized (diagonal) control algorithms of the lowest possible order. These practices are necessary due to stringent implementation and calibration constraints. Hence, the effectiveness or potential fundamental limitations of decentralized controllers as well as the role of controller order are also considered for the current problem.

A. Decentralized structure

We consider the proposed decentralized controller $C = \text{diag}(C_{11}, C_{22})$ that is depicted in figure 5. The wheel speed is given by

$$\omega_w(s) = \frac{\alpha_r P_{21} C_{11} + P_{22} C_{22} + P_{11} C_{11} P_{22} C_{22}}{(1 + P_{11} C_{11})(1 + P_{22} C_{22})} \tilde{\alpha}_p. \quad (9)$$

Let C_{11} and C_{22} be causal and realizable controllers that achieve closed loop stability. For minimum phase behavior we require that the initial value of the derivative of the wheel speed is positive during a step change in pedal position command,

$$\dot{\omega}_w(t=0) = \lim_{s \rightarrow \infty} s^2 \omega_w(s) > 0. \quad (10)$$

In the limit as $s \rightarrow \infty$ the denominator of $\omega_w(s)$ in Eq (9) is 1. After applying a unit step input, the limit as $s \rightarrow \infty$ for the numerator of $s^2 \omega_w(s)$ is

$$\lim_{s \rightarrow \infty} s(\alpha_r P_{21} C_{11} + P_{22} C_{22} + P_{11} C_{11} P_{22} C_{22}). \quad (11)$$

For stability and steady-state tracking reasons C_{11} must have positive coefficients. It is thus not possible to change the sign of the component of the initial response that contributes to the inverse behavior ($\alpha_r P_{21} C_{11}$) by manipulating the sign of the controller C_{11} . Consequently, the initial

wheel speed response is dominated by the path with the smallest pole-zero excess, relative degree (rd), or the fewest number of integrations.

From Eq (6) and figure 2, the relative degree of each portion of the system transfer function can be determined as $rd(P_{11}) = 1$, $rd(P_{21}) = 1$, and $rd(P_{22}) = 2$. Due to its high relative degree, the component $P_{11}C_{11}P_{22}C_{22}$ does not contribute to the initial response. To compensate the inverse response due to the NMP zero in P_{21} , it is important to design a decentralized controller so that the relative degree of the upper path (through the NMP contributions) is larger than the relative degree of the lower path,

$$\begin{aligned} rd(P_{21}C_{11}) &\geq rd(P_{22}C_{22}) \Rightarrow \\ rd(P_{21}) + rd(C_{11}) &\geq rd(P_{22}) + rd(C_{22}) \Rightarrow \\ rd(C_{11}) &\geq rd(C_{22}) + 1. \end{aligned} \quad (12)$$

As one can see, a proportional (P), proportional-integral (PI) diagonal controller does not satisfy condition 12. We are interested in the P,PI controller because it provides the lowest order decentralized controller that permits output tracking with zero steady state error. Indeed, because the ratio output is the integral of the ratio rate input, a proportional feedback gain for this loop suffices to track the desired reference ratio, r^o . For the wheel speed to track the desired reference, ω_w^o , C_{22} must include an integrator.

Note that condition 12 is satisfied if C_{11} is a lag. Introducing a lag in the C_{11} term will eliminate the inverse response of the ω_w but can potentially slow down the closed-loop response in the upper loop. A similar effect can be achieved if we prefilter the command α_r before the feedback loop. This result sheds light on an important limitation of the decentralized controller architecture. Namely, a decentralized controller imposes a tradeoff between fast ratio rate and initial monotonic wheel speed response.

Another important observation is that if the breathing dynamics is negligible in the P_{22} term then the relative degree condition for the minimum phase (MP) response is modified,

$$rd(C_{11}) \geq rd(C_{22}). \quad (13)$$

The new condition is satisfied by a P,PI decentralized controller without the need to slow down the upper loop. As one expects, fast dynamics from $\theta \rightarrow \omega_w$ can potentially compensate for the initial inverse response from $\dot{r} \rightarrow \omega_w$. This has also been verified numerically.

B. Multivariable

It is of interest to investigate if a fully centralized multivariable controller can mitigate the tradeoff between fast ratio rate and monotonic initial wheel speed associated with the decentralized controller architecture that we analyzed in the previous section. When a fully centralized multivariable controller is considered for the TITO system the wheel speed is given by

$$\omega_w = \frac{P_{21}(\alpha_r C_{11} + C_{12}) + P_{22}(\alpha_r C_{21} + C_{22}) + P_{11}P_{22}(C_{11}C_{22} - C_{12}C_{21})}{1 + P_{11}C_{11} + P_{21}C_{12} + P_{22}C_{22} + P_{11}P_{22}(C_{11}C_{22} - C_{12}C_{21})} \tilde{\alpha}_p. \quad (14)$$

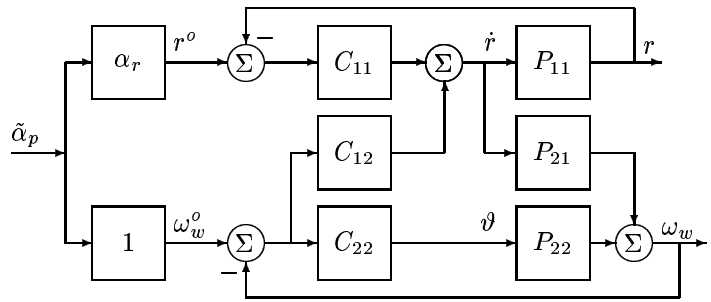


Fig. 6. The reduced multivariable controller (where $C_{21} = 0$) with the TITO system

The lowest order multivariable controller that achieves the steady-state tracking requirement uses P,P,P,PI for the C_{11} , C_{12} , C_{21} , C_{22} controllers, respectively. For minimum phase behavior we require that the initial value of the derivative of the wheel speed is positive during a step change in pedal position command, as in Eq (10). In the limit as $s \rightarrow \infty$ the denominator of $\omega_w(s)$ is again 1. After applying the step input the numerator of $s^2\omega_w(s)$ is

$$\lim_{s \rightarrow \infty} s [P_{21}(\alpha_r C_{11} + C_{12}) + P_{22}(\alpha_r C_{21} + C_{22}) + P_{11}P_{22}(C_{11}C_{22} - C_{12}C_{21})]. \quad (15)$$

Using the plant in Eq (6) the initial wheel acceleration is defined by

$$\dot{\omega}_w(t=0) = g_1(x^o)(\alpha_r C_{11} + C_{12}). \quad (16)$$

By choosing C_{11} and C_{12} such that

$$\alpha_r C_{11} + C_{12} \leq 0 \quad (17)$$

the initial inverse response caused by the NMP zero in P_{21} can be eliminated independently of the order of the multivariable controller or the methodology for its design. Thus, the following summarizes the important points:

- (i) The multivariable controller does not present any limitation in achieving fast ratio rate response and a monotonic initial wheel speed.
- (ii) The C_{12} term is the important cross coupling term that enables the multivariable controller to mitigate the limitations of the decentralized architecture. It provides the mechanism with which the ratio rate command utilizes the errors of both outputs to avoid degradation in the lower loop.

The structure of the controller interaction with the plant is shown in figure 6.

To illustrate these findings, one set of fixed gains for the P,P,P,PI multivariable controller is found to compensate the linearized system for various steps of driver pedal positions. In particular, the constants are chosen such that $\alpha_r C_{11} + C_{12} = 0$. The time responses are plotted in figure 7 as the heavy solid lines, showing no initial inverse for either the wheel speed or ratio and very good performance. The different step sizes are 10 – 20%, 60 – 75%, 30 – 90%, and 10 – 99%. The 60 – 75% step response is comparable to the example command used in [10]. Notably, increasing the step size causes the response to overshoot. With

some tuning, the gains can be scheduled for various step sizes over different operating conditions to optimize each time response. The lighter lines in these plots represent the nonlinear system compensated by the same linear controller with the same fixed gains in response to the same 4 different driver pedal positions. For smaller step commands, such as the 10 – 20% and 60 – 75%, the linearized and nonlinear system output responses are indistinguishable. When the step command is large, the nonlinear system response is significantly slower than the linearized system response.

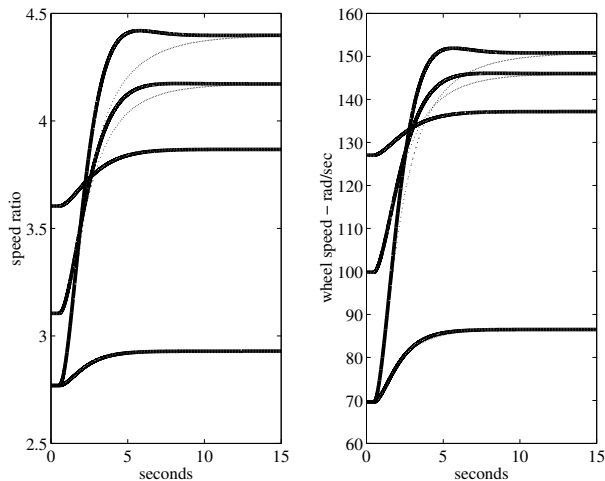


Fig. 7. Ratio and wheel speed time responses to different “kick-down” maneuvers

The phase trajectories from the nonlinear simulations are plotted in figure 8 on the engine characteristics map. By relaxing the requirement to maintain optimum engine operations, the unconstrained mass air flow causes the engine transient to deviate from the $\Gamma(\omega_e(t))$ curve. Remarkably, despite the use of the lowest order linear tracking multivariable controller with fixed gains for all operating conditions, the deviation is not very large even for large step commands. The heavy dashed and jagged line is a comparison of a 10-20% pedal position response of a conventional automatic transmission which does not satisfy the $\Gamma(\omega_e(t))$ curve even at steady state.

VIII. CONCLUSIONS

This investigation shows that the SITO approach, which guarantees the engine to operate on the prescribed $\Gamma(\omega_e(t))$ curve, always results in initial wheel speed undershoot in response to a step driver pedal position command. By relaxing the transient engine operating requirement to stay on the $\Gamma(\omega_e(t))$ curve, the throttle can be used to compensate this wheel speed initial undershoot. But the lowest order decentralized tracking controller with the TITO approach cannot achieve both a stable and monotonic wheel speed response. A decentralized controller that achieves the desired wheel speed performance must slow down the ratio controller. Alternatively, an appropriate choice for the off-diagonal term, C_{12} , of the multivariable controller can cancel the nonminimum phase effect of ratio rate on

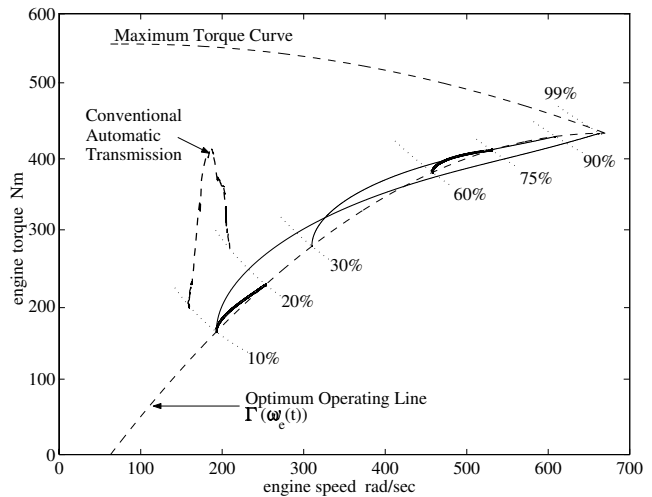


Fig. 8. Phase portrait of simulated responses on the engine characteristics map

the wheel speed initial response without slowing down the ratio controller. In fact, the lowest order constant linear multivariable tracking controller is shown for various examples to achieve good wheel acceleration performance without significantly deviating from the transient objective, the $\Gamma(\omega_e(t))$ curve. Experimental verification and robustness analysis of the multivariable TITO controller will be pursued in future work.

ACKNOWLEDGMENTS

This work is supported by the National Science Foundation under contract ECS-0049025. We also thank GM for the continuing support throughout the first author’s PhD studies.

REFERENCES

- [1] Fitz, Frank A. and Paul B. Pires, Epilogics, Inc. *A high torque, high efficiency CVT for electric vehicles*, SAE Paper 910251.
- [2] Fitz, Frank A. and Paul B. Pires, Epilogics, Inc. *A geared infinitely variable transmission for automotive applications*, SAE Paper 910407.
- [3] Kemper, Yves and Lee Elfes, Vadatec Corp. *A continuously variable traction drive for heavy-duty agricultural and industrial applications*, SAE Paper 810948.
- [4] Smith, M.J., C.J. Greenwood, and G.B. Soar, *A full-toroidal traction drive CVT - from theory to practice*, International Mechanical Engineer, 1992, C389/066, 925061.
- [5] Hirano, Sadayuki, Alan L. Miller, and Karl F. Schneider, *SCVT - A state of the art electronically controlled continuously variable transmission*, SAE Paper 910410.
- [6] Vahabzadeh, Hamid and Samuel M. Linzell, *Modeling, simulation, and control implementation for a split-torque, geared neutral, infinitely variable transmission*, SAE Paper 910409.
- [7] Funatsu, Koichi, Hideo Koyama, and Takashi Aoki, *Electronic control system of Honda for CVT*, International conference on Continuously Variable Power Transmissions CVT 1996, Yokohama Proceedings, Sept. 11-12, 1996, (Conf. Pub. No. 107).
- [8] Yasuoka, Masayuki, Masaaki Uchida, Shusaku Katakura, and Takahiro Yoshino, *An integrated control algorithm for an SI engine and a CVT*, SAE Paper 1999-01-0752.
- [9] Deacon, M., C.J. Brace, M. Guebeli, N.D. Vaughan, C.R. Burrows, R.E. Dorey, *A modular approach to the computer simulation of a passenger car powertrain incorporating a diesel engine and continuously variable transmission*, IEE International Conference on Control 1994, London, UK, vol. 1, no. 389.

- [10] Guzzella, Lino and Andreas Michael Schmid, *Feedback linearization of spark-ignition engines with continuously variable transmissions*, IEEE Transactions on Control Systems Technology, Vol. 3, no.1, March 1995, pp. 54-60.
- [11] Schmid, Andreas, Philipp Dietrich, Simon Ginsburg, and Hans P. Geering, *Controlling a CVT-equipped hybrid car*, SAE Paper 950492.
- [12] Gott, Philip G., *Changing Gears: The Development of the Automotive Transmission*, SAE, Inc., 1991.
- [13] Newton, K., W. Steed, T.K. Garrett, *The Motor Vehicle*, 12th ed., SAE International, Warrendale, PA, 1996, pp. 716, 737-743.
- [14] Chan, C., D. Yang, T. Volz, D. Breitweiser, F.S. Jamzadeh, A. Frank, and T. Omitsu, *System design and control considerations of automotive continuously variable transmissions*, SAE Paper 840048.
- [15] Engelsdorf, Kurt, Karl-Heinz Senger, Martin-Peter Bolz, *Electronic CVT control for power train optimization*, International conference on Continuously Variable Power Transmissions CVT 1996, Yokohama Proceedings, Sept. 11-12, 1996, (Conf. Pub. No. 111).
- [16] Liebrand, Nort, *Future Potential for CVT Technology*, International conference on Continuously Variable Power Transmissions CVT 1996, Yokohama Proceedings, Sept. 11-12, 1996, (Conf. Pub. No. 105).
- [17] Smith, M.J., D.H. Ridmarsh, and P. Foss, *The development of high specific output engines for use with a two regime IVT*, Autotech 1993, NEC Birmingham UK C427/36/237.
- [18] Seron, Maria M., Julio H. Braslavsky, and Graham C. Goodwin, *Fundamental Limitations in Filtering and Control*, Springer, 1997.
- [19] Freudenberg, Jim, Rick Middleton, Anna Stefanopoulou, *A Survey of Inherent Design Limitations*, American Control Conference Workshop Tutorial 2000, Chicago, IL, June 2000.
- [20] Stefanopoulou, A.G., K.R. Butts, J.A. Cook, J.S. Freudenberg and J.W. Grizzle, *Automotive Powertrain Control for Modular Controller Architectures: A Case Study*, Proc. 1995 Conference on Decision and Control, pp. 768-773.
- [21] Kim, Hyunsoo, Hanlim Song, Talchol Kim, and Jongjum Kim, *Metal Belt CVT and Engine Optimal Operation by PWM Electro-Hydraulic Control*, International conference on Continuously Variable Power Transmissions CVT 1996, Yokohama Proceedings, Sept. 11-12, 1996, (Conf. Pub. No. 304).
- [22] Bosch Automotive Handbook, 3rd. edition, 1994.
- [23] Marcopoli, V., *Inherent limitations associated with the weapon pointing control problem for a tank elevation system*, Proceedings of the 2000 American Control Conference, Chicago, IL, June 2000.
- [24] Middleton, R.H., *Tradeoffs in linear control system design*, Automatica, Vol. 27, no.2, pp. 281-292, 1991.
- [25] Shafai, Esfandiar and Hans Geering, *Control issues in a fuel-optimal hybrid car*, 1996 IFAC 13th Triennial World Congress, San Francisco, USA, Session 8b-07 4, pp. 231-236.
- [26] Serranrens, Alex, Bas Vroemen, *CVT Control: A Hierarchical Approach*, Proceedings of ASME AVEC 2000, Ann Arbor, MI, USA, No. 134 pp.
- [27] Shen, Shuiwen, A.F.A. Serranrens, M. Steinbuch, F.E. Veldpaus, *Control of a Hybrid Driveline for Fuel Economy and Driveability*, Proceedings of ASME AVEC 2000, Ann Arbor, MI, USA, No. 68 pp.

APPENDIX

Assume there is no slip across the entire powertrain. The speed ratio is defined in Eq (1) as

$$r = \frac{\omega_e}{\omega_w} = \left(\frac{T_{eb}}{T_w}\right)^{-1}. \quad (18)$$

Its time derivative is

$$\dot{\omega}_e = \dot{r}\omega_w + r\dot{\omega}_w. \quad (19)$$

Fit the indicated/generated torque as a 2nd order polynomial function in engine speed,

$$T_{ind} = c_1 + c_2 m_a + c_3 \omega_e + c_4 \omega_e^2. \quad (20)$$

The brake torque, the input to the transmission, is the indicated torque minus viscous losses and engine inertia as expressed in Eq (2),

$$\begin{aligned} T_{eb} &= T_{ind} - c_{ef}\omega_e^2 - I_e\dot{\omega}_e \\ &= c_1 + c_2 m_a + c_3 \omega_e + (c_4 - c_{ef})\omega_e^2 - I_e\dot{\omega}_e \end{aligned} \quad (21)$$

The torque driving the wheels is the car inertia plus car load in Eq (4),

$$\begin{aligned} T_w &= I_w\dot{\omega}_w + T_l \\ &= I_w\dot{\omega}_w + C_F W_c \cos \beta + W_c \sin \beta + C_D \omega_w^2. \end{aligned} \quad (22)$$

The car load consists of tire friction, driving surface grade, and air drag, $T_l = C_F W_c \cos \beta + W_c \sin \beta + C_D \omega_w^2$. Using the far right-hand side of Eq (1),

$$T_w = rT_{eb}, \quad (23)$$

substitute the preceding expressions of torque into the torque ratio and eliminate the engine speed to get this expression,

$$\begin{aligned} I_w\dot{\omega}_w + C_F W_c \cos \beta + W_c \sin \beta + C_D \omega_w^2 &= \\ (c_1 + c_2 m_a)r + c_3 r^2 \omega_w + (c_4 - c_{ef})r^3 \omega_w^2 - I_e r \dot{\omega}_e. \end{aligned} \quad (24)$$

Substituting Eq (19) for engine acceleration, this expression can be arranged with wheel acceleration terms only on the left-hand side.

$$\begin{aligned} (I_w + I_e r^2)\dot{\omega}_w &= (c_1 + c_2 m_a)r + c_3 r^2 \omega_w + (c_4 - c_{ef})r^3 \omega_w^2 \\ &\quad - (C_F W_c \cos \beta + W_c \sin \beta) - C_D \omega_w^2 - I_e r \omega_w \dot{r}. \end{aligned} \quad (25)$$

This yields the standard equation of motion for wheel acceleration of a CVT powertrain,

$$\begin{aligned} \dot{\omega}_w &= \frac{[(c_4 - c_{ef})r^3 \omega_w^2 - C_D]\omega_w^2 + c_3 r^2 \omega_w + [(c_1 + c_2 m_a)r - \bar{\beta}]}{I_w + I_e r^2} \\ &\quad - \frac{I_e r \omega_w}{I_w + I_e r^2} \dot{r}, \end{aligned} \quad (26)$$

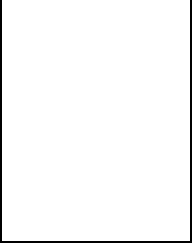
that is \dot{x}_2 in Eq (5) when the states are $x = [r \ \omega_w \ m_a]^T$, and $\bar{\beta} = C_F W_c \cos \beta + W_c \sin \beta$. If m_a is pre-determined as in the SITO case and \dot{r} is the only input, u , then letting

$$\begin{aligned} \gamma &= c_1 + c_2 m_a & a &= C_D & \nu &= r \\ \alpha &= c_4 - c_{ef} & \beta' &= c_3 & \Theta_e &= I_e \\ c &= \bar{\beta} & \eta &= 1 & \Theta_w &= I_w \end{aligned} \quad (27)$$

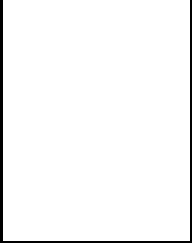
turns Eq (26) into

$$\dot{\omega}_w = \frac{[\alpha\nu^3 - a]\omega_w^2 + \beta'\nu^2\omega_w + [\gamma\nu - c]}{\Theta_w + \Theta_e\nu^2} - \frac{\Theta_w\nu\omega_w}{\Theta_w + \Theta_e\nu^2}u, \quad (28)$$

which is exactly Eq (4) of [10].



Anna G. Stefanopoulou obtained her Diploma (1991, Nat. Tech. Univ. of Athens, Greece) and M.S. (1992, Univ. of Michigan, U.S.) in Naval Architecture and Marine Engineering. She received her second M.S. (1994) and her Ph.D. (1996) in the University of Michigan, Electrical Engineering and Computer Science department. Dr. Stefanopoulou is presently an associate professor at the Mechanical Engineering department at the University of Michigan. She was an assistant professor at the University of California, Santa Barbara, and a technical specialist at the Scientific Research Laboratories at Ford Motor Company. Dr. Stefanopoulou is Chair of the Transportation Panel in ASME DSCD, a recipient of a 1997 NSF CAREER, a 1998 and 2000 Ford Innovation award, a 1999 UCSB SPUR Undergraduate Research Mentor Award, and a 2002 SAE Ralph R. Teetor Educational Award. She has also participated the 1999 NAE and 2001 Alexander von Humboldt Foundation (AvH) Frontiers of Engineering Symposia. Her research interests are in multivariable feedback control, controller architectures for industrial applications, and powertrain control.



Sharon Liu obtained her B.S.E. (1989, Duke University, N.C., USA) with a concentration in Material Science, M.S. (1993, Stanford University, C.A., USA) with a concentration in Product Design, and Ph.D. (1999, University of California, Santa Barbara, C.A., USA) in the Mechanical and Environmental Engineering Department, the Dynamics and Controls Group. Presently, she works at Advanced Propulsion System Controls, General Motors Powertrain, Milford, MI, USA.